Supramolecular Complex of Poly(styrene)-b-Poly-(4-vinylpyridine) and 1-Pyrenebutyric Acid in Thin Film

Biplab K. Kuila, Manfred Stamm**

Summary: Here, we have described a novel supramolecular complex (SMC) between poly-(styrene)-b-poly(4-vinylpyridine) (PS-b-P4VP) and 1-pyrenebutyric acid (PBA) and studied of its self assembly in thin film. PBA will make supramolecular complex with the P4VP block due to strong hydrogen bonding between the carboxylic group of 1-pyrenebutyric acid and pyridine ring of P4VP. The formation of supramolecular complex between PS-P4VP and PBA through hydrogen bonding is investigated through FTIR study. The supramolecular complex of PS-b-P4VP and 1-pyrenebutyric acid changed the block copolymer morphology from cylindrical to lamella in thin film due to the increase of the volume fraction of P4VP (PBA). In both cases (parent block copolymer and SMC), the microdomains are oriented normal to the substrate after annealing in a selective solvent. Pure block copolymer shows cylindrical morphology with a periodicity of $\sim$26 nm, whereas the SMC shows lamellar morphology with a periodicity of $\sim$ 29 nm. After fabricating the thin film from SMC, 1-pyrenebutyric acid can be easily removed by dissolving the thin film in ethanol to transform the block copolymer thin film into nanotemplate or membrane.

Keywords: block copolymer; Hydrogen bonding; self assembly; supramolecular complex

Introduction

Self-assembly of block copolymers (BCP) are the focus of intensive research attention in the field of nanoscience and nanotechnology due to their tendency to form a wide range of periodic structures in the nanoscopic length scale.[1–5] BCP can self assemble into a variety of nanoscale structures (spherical, cylindrical, gyroidal, lamellar) with dimensions from a few nanometres to above 100 nm depending on molecular weight, segment size, and the strength of interaction between the blocks, represented by the Flory–Huggins interaction parameter, χ. In most of the practical applications block copolymers are used in the form of thin films and the structural behavior of BCP thin films compared with bulk materials is often much more complicated due to the interfacial interactions of the blocks with the underlying substrate, the surface energies of the blocks and commensurability with the film thickness. Significant progress has been made in controlling the microdomain orientation and long-range order in BCP thin films.[5–8] This class of ordered materials are promising for applications[9–12] in many fields of nanoscience and nanotechnology such as surface patterning, lithography and templating for the fabrication of ordered arrays of metal, magnetic, polymeric, semiconducting nanomaterial of high density (terabits per cm^2) used for electronic, electrochemical, optoelectronic, magnetic, photonic, and biosensing device applications.

Recently, it was demonstrated that self assembly of block copolymer supramolecular complex is a simple and powerful technique for fine tuning of the block copolymer morphologies, and has been successfully applied in bulk[13–15] and in

Department of Nanostructured Materials, Leibniz Institute of Polymer Research Dresden, Hohe Strasse 6, D-01069 Dresden, Germany
E-mail: stamm@ipfdd.de, biplab.kuila@yahoo.com

thin films.[16–18] In this approach, a low molar mass additive is attached with one of the blocks by noncovalent interactions such as metal coordination, hydrogen bonding, Van der Waals forces, π-π interactions and electrostatic effects.[15–25] These supramolecular complexes offer advantages over the covalently linked analogues, since different functionalities can be introduced into the assemblies simply by substituting the small molecules, thereby avoiding the need to synthesize entirely new families of BCP.[25,26] This will reduce the burden of synthesizing entirely new families of BCP with greater functionality. Another major advantage of block copolymer supramolecular complex strategy is that the low molar mass additive after thin film formation can be removed easily by selective dissolution to obtain a nanoporous material.[16,18] These nanopores and nanochannels that are lined with functional groups are readily available for further applications. Among various types of supramolecular complexes, those containing hydrogen bonds hold a prominent place in supramolecular chemistry because of their directionality and versatility. The pioneering groups of Ikkala and ten Brinke have first demonstrated the preparation of hierarchical polymeric materials through the complexation of 3-pentadecyl phenol (PDP) and poly-(styrene)-block-poly(4-vinylpyridine) (PS-P4VP) in bulk by hydrogen bonds.[13,26,27] The resultant complexes display a structure-within-structure pattern characterized by two length scales. Most of the studies using PDP as a low molar mass additive to form SMC with block copolymer have focused on the bulk and recently, there are few reports on thin films of PS-P4VP (PDP) based supramolecular complexes. These studies mainly focused on the morphology, phase behaviour and terrace formation of the SMC thin film.[17,28,29] Very recently, Tung et al.[28] systematically studied PS-*b*-P4VP (PDP) with a wide range of P4VP(PDP) weight fraction and established a correlation between orientation of supramolecular complexes in thin films and the weight fraction of P4VP (PDP). Also they demonstrated the formation of hierarchical assemblies, e.g., lamella-within-lamella and cylinders-within-lamella in thin films.

Our group[16,18] in past few years has worked extensively on block copolymer SMC mostly with an aim to fabricate polymer nanotemplates for further nanofabrication. One of the systems widely studied by us consists of SMCs formed by poly(styrene)-*b*-poly(4- vinylpyridine) (PS-*b*-P4VP) and 2-(4′-hydroxybenzeneazo) benzoic acid (HABA) where P4VP(HABA) comb block forms cylindrical microdomains surrounded by PS matrix. This supramolecular system shows the reversible switching of the orientation of the microdomains (for example: parallel cylinder to perpendicular cylinder) upon exposure to solvent vapours. Selective extraction of HABA creates pores or polymeric nano-objects which we used as templates for nanofabrication. It is worth mentioning here that the uniform film formation and the homogeneous distribution of HABA molecules in SMC thin films are very sensitive to the film deposition conditions. It was noticed that if the interaction between block copolymer and small molecules is not strong enough to form comb like structure, additive will come out from the thin film and crystallizes on the surface of the thin film during annealing and hampers the order and orientation of the microdomains.[30] Considering these difficulties, limited numbers of reports are available on the study of block copolymer based SMC in thin films and in most of these studies PDP or HABA were used as a low molar mass additive to form the hydrogen-bonding. It is necessary to add new additives to the library of PS-*b*-P4VP based SMC for the complete understanding of constrains or factors which control the block copolymer supramolecular assembly and the orientation of the microdomain in thin film. In this manuscript, we have studied the self assembly of a novel block copolymer supramolecular complex consist of 1-pyrenebutyric acid and PS-b-P4VP. 1-pyrenebutyric acid

(PBA) is an important photoluminescence molecule used as fluorescent dye and electroluminescent dopant. PBA forms SMC with the P4VP block due to strong hydrogen bonding between the carboxylic group of 1-pyrenebutyric acid and pyridine ring of P4VP. The SMC of PS-b-P4VP with 1-pyrenebutyric acid resulted in changing of the cylindrical nanodomain of block copolymer into lamella in thin film due to compositional change. After fabricating the thin film from the self assembly of the supramolecular complex, 1-pyrenebutyric acid can be easily removed by dissolving the thin film in ethanol to transform the block copolymer thin film into nanotemplate or membrane.

Experimental Part

Materials

PS (32900)-*b*-P4VP (8000) (PDI = 1.06) was purchased from polymer source inc. 1-*pyrenebutyric acid* (PBA) (97%), was purchased from Aldrich Sigma Chemicals. The solvents 1,4-Dioxane, Chloroform, Tetrahydrofuran(THF), ethanol, and dichloromethane were purchased from Acros Organics and used as it is. Silicon wafers {100} were cleaned successively in an ultrasonic bath (dichloromethane) for 15 min and a ''piranha'' bath (30% H_2O_2, 70% of H_2SO_4, *chemical hazard*) for 90 min at 75 °C, and then thoroughly rinsed with Millipore water and dried under an argon flow.

Fabrication of Nanotemplate

PS-b-P4VP and PBA (1 mol of PBA: 1 mol of 4-vinylpyridine monomer unit) were dissolved separately. PS-b-P4VP solution was then added drop-by-drop to PBA solution, while the solution was heated close to the boiling point of the solvent in an ultrasonic bath. The resulting complex solution (the total concentration PS-b-P4VP + PBA 1% (w/v)) was kept overnight to complete hydrogen bonding formation. Thin films of PS-b-P4VP + PBA were prepared by dip-coating method from the filtered composite solutions at rate of 1 mms^{-1}. Dip-coated thin films were further annealed in saturated vapours of 1,4–Dioxane for 4 days to improve the order of the nanodomains. Selective extraction of PBA from PS-b-P4VP + PBA thin film leads to the formation of block copolymer nanotemplate.

Characterization of the Block Copolymer Thin Films

Thickness

The thickness of the polymer films on silicon substrate was measured by an SE 400 ellipsometer (SENTECH Instruments GmbH, Germany) with a 632.8 nm laser at a 70° incident angle.

FTIR

Block copolymer thin films deposited on cleaned silicon wafers were directly used for FTIR measurements. Infrared spectra were recorded with a Bruker IFS 66v FTIR spectrometer in the reflectance mode.

GISAXS

GISAXS measurements were carried out at the beamline BW4 of the DORIS III storage ring at HASYLAB (DESY, Hamburg, Germany). The X-ray wavelength was $\lambda = 0.138$ nm. The sample was placed horizontally on a goniometer. Two beam stops were used in these measurements. One beam stop was used to block the direct beam and a second one to block the very high specular intensity on the detector. The incident angle was set to $\alpha_i = 0.20°$, which is well above the critical angles of the polymer (0.16°), but below the critical angle for Si (0.22°). Therefore, the X-ray beam penetrates the whole film and the scattering data gives the information of the structural lengths present in the full depth of the film. The scattered intensities were recorded by a 2D detector (MARCCD; 2048×2048 pixel). Line averaged intensities are reported as I vs q, where $q = (4\pi/\lambda)\sin(\theta/2)$, λ is the wavelength of incident X-rays, and θ is the scattering angle.

AFM

The AFM imaging was performed on as prepared samples on silicon or glass substrate by a Dimensions 3100 (NanoScope IV – Controller) scanning force microscope in the tapping mode. The tip characteristics are as follows: spring constant 1.5-3.7 Nm^{-1}, resonant frequency 45-65 KHz, tip radius about 10 nm.

FESEM

FESEM images were obtained with field emission electron microscopy (Zeiss Ultra 55 Gemini with FIB) operating at 3 kV. The samples were investigated without staining and the working distance was 3 mm.

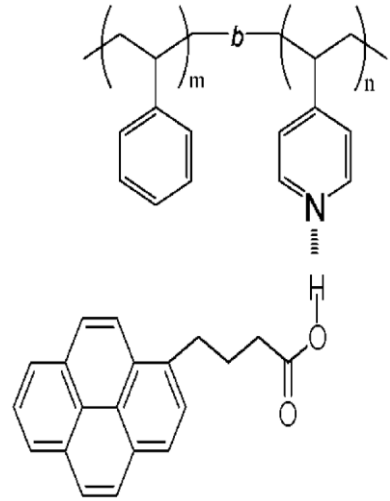

Figure 1.
Chemical drawing of the SMC formation through hydrogen bonding between P4VP block of PS-*b*-P4VP copolymer and PBA.

Results and Discussion

Block copolymer supramolecular complex thin films based on PS-b-P4VP and PBA were deposited on cleaned silicon wafers by dip-coating from 1% complex solution in 1,4-Dioxane. Under an optical microscope, the polymer films with thicknesses about 30 nm are macroscopically and microscopically smooth and show no signs of PBA phase separation, such as crystals or stains. This may clearly suggest that PBA molecules are associated with P4VP blocks building comblike polymer chains. The chemical structure of the PS-*b*-P4VP (PBA) supramolecular complex is shown in Figure 1.

The supramolecular complex formation between PS-b-P4VP and PBA was investigated by FTIR. Figure 2 (Figure 2a from 1050 to 980 cm^{-1} and Figure 2b from 1900 to 1615 cm^{-1}) shows the FT-IR spectra of PBA, PS-*b*-P4VP and PS-b-P4VP (PBA) thin films before and after washing in ethanol. Free pyridine groups in the PS-*b*-P4VP thin film contribute to the absorption at 994 cm^{-1} [14,15] (which is absent in PBA spectra). As seen from Figure 2a the intensity of the absorption peak at 994 cm^{-1} disappears in PS-b-P4VP (PBA) thin film and a new broad peak appears at 1014cm^{-1} which is due to the hydrogen bonded pyridine ring,[19,20,26] confirming the formation of supramolecular complex between PS-b-P4VP and PBA through hydrogen bonding (see Figure 1). The formation of hydrogen bonding is further confirmed by the band at 1695 cm^{-1}, which is corresponding to the stretching frequency of C=O bond from carboxylic acid group of PBA. As seen in Figure 2b this band shifted to higher wave number at 1709 cm^{-1} in PS-P4VP (PBA) due to hydrogen bonding between carboxylic group of PBA and pyridine ring of PS-b-P4VP. After immersing the PS-b-P4VP (PBA) thin film in ethanol, the free pyridine peaks are recovered, whereas the characteristic peaks of PBA have disappeared as shown in particular by the stretching frequency of C=O bond from carboxylic acid group of PBA at 1695 cm^{-1}. This indicates that washing with ethanol is an efficient way to eliminate PBA from the thin film of PS-b-P4VP/ PBA supramolecular complex to generate nanotemplates.

The PS (32900)-*b*-P4VP (8000) (PDI = 1.06) block copolymer used here exhibits cylindrical morphology in bulk where the P4VP core is surrounded by PS matrix. Block copolymer thin films were prepared by dip-coating process using 1%

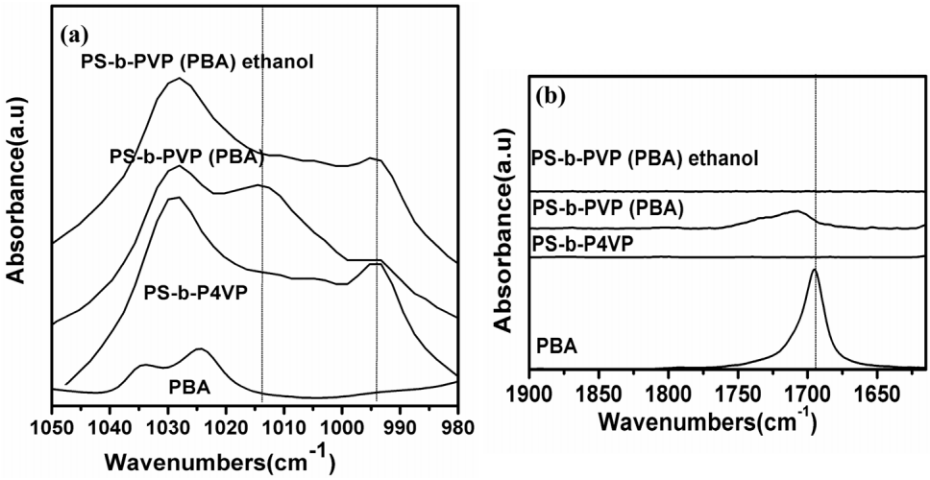

Figure 2.
FT-IR spectra of PBA, PS-*b*-P4VP, PS-*b*-P4VP+PBA and ethanol washed PS-*b*-P4VP+PBA thin film in different region (a) 1050 - 980 cm^{-1} (b) 1900 – 1615 cm^{-1}.

PS-*b*-P4VP solution in 1,4-Dioxane. Figure 3 shows the atomic force microscope height images of the samples after solvent annealing in 1,4-Dioxane and the corresponding structures after the surface reconstruction (rinsing with ethanol). The AFM images of as dip-coated films of pure block copolymers showed disordered cylindrical microdomains due to fast solvent evaporation, leaving the chains insufficient time to rearrange to attain ordered morphology. 1,4-Dioxane vapour annealed thin films assemble into hexagonally packed cylindrical microdomains oriented normal to the substrate (Figure 3a). When the solvent annealed films were immersed into ethanol, a good solvent for P4VP and a non-solvent for PS, a surface reconstruction of the films is observed with a fine structure (Figure 3b). Russell and co-workers have shown such a surface reconstruction process in PS-*b*-P4VP diblock copolymer thin films and demonstrated that the preferential solvation of P4VP blocks with ethanol does not alter the order or orientation of the microdomains.[31] Surface reconstruction of a 1,4-Dioxane annealed film of pure block copolymer keeps the well-developed microdomain structure, having hexagonal order with an average center-to- center spacing of ≈26 nm and pore diameter of ≈12 nm (Figure 3b). On the other hand, PBA added SMC thin films showed different morphology as compared to the parent block copolymer thin film as shown in Figures 3c-d because of the selective interaction of PBA with P4VP blocks. A dip-coated thin film of SMC does not show any characteristic morphology. This morphology is kinetically trapped and far from the equilibrium due to the fast removal of the solvent during dip-coating. On further annealing these SMC thin films in 1,4-Dioxane vapours leads to structural reorganization to lamellar structure and the lamellae are oriented normal to the substrate as shown in Figure 3c. The surface reconstruction as well as the removal of PBA was done by dipping the SMC thin film in ethanol similar to the case of pure block copolymer. Figure 3d shows the AFM image of the SMC thin film on silicon substrate after surface reconstruction that demonstrates distinct lamella domains normal to the substrate (Figure 3d) with spacing of ≈29 nm. The complete removal of the PBA is proved by the FTIR as discussed in the preceding section. In order to further confirm the morphology observed by AFM, we have performed the FESEM study. Figure 4 shows the SEM images of nanotemplates from pure block

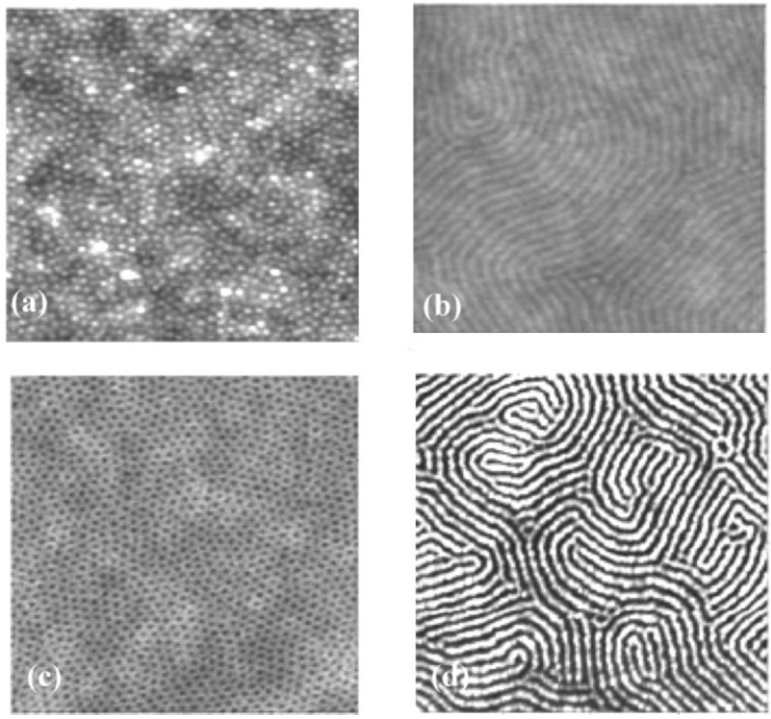

Figure 3.
AFM height images of (a) PS-b-P4VP block copolymer thin film after 1,4-Dioxane vapour annealing (b) 1,4-Dioxane vapour annealed block copolymer thin film after surface reconstruction (c) thin film from SMC with PBA after 1,4-Dioxane vapour annealing (d) 1,4-Dioxane vapour annealed SMC thin film after surface reconstruction.

copolymer and from a supramolecular complex after surface reconstruction. SEM results are in good correlation with the AFM results. The block copolymer nanotemplate shows hexagonally packed cylindricaly channels perpendicular to the silicon substrate, whereas the SMC template reveals perpendicular lamellar structure.

AFM and SEM give the surface morphology of the thin films; however neither of these techniques allowed us to under-

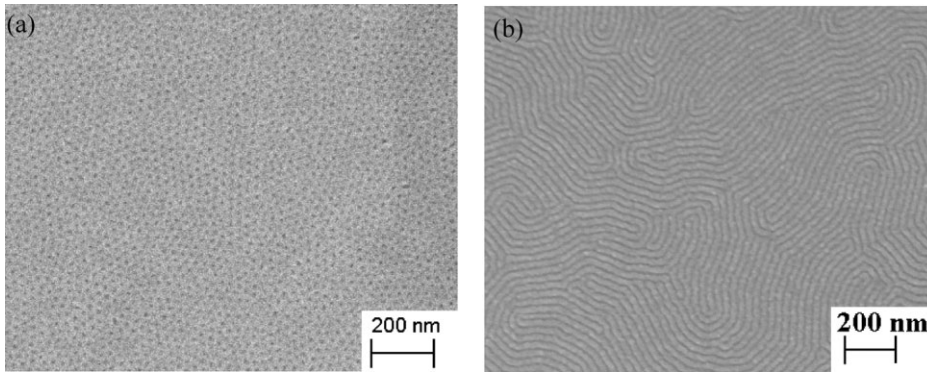

Figure 4.
(a) pure block copolymer thin film after surface reconstruction (b) SMC thin film after surface reconstruction.

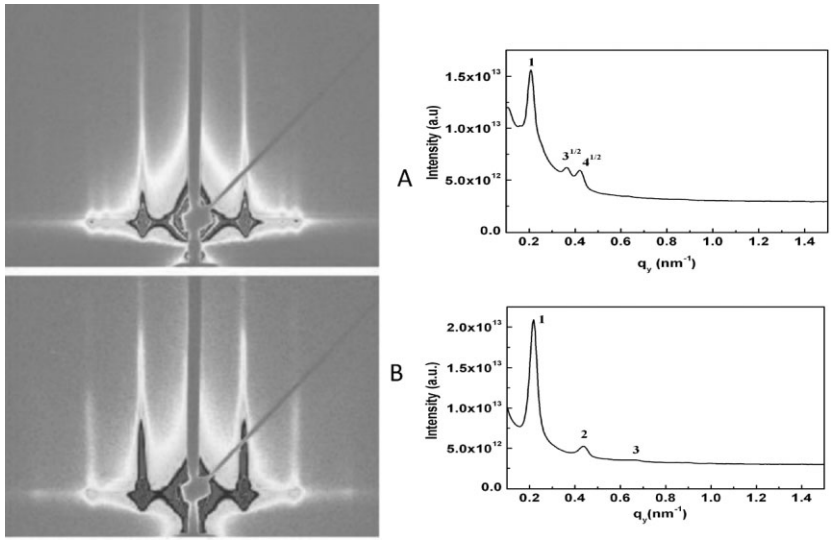

Figure 5.
2D GISAXS patterns and their corresponding in-plane intensity profiles. (A) Surface reconstructed PS-*b*-P4VP nanoporous template (B) 1,4-dioxane annealed SMC template after the removal of PBA.

stand the buried structures inside the thin films. GISAXS is a powerful technique to investigate the internal morphology of thin films. Figure 5 shows the GISAXS patterns measured for two samples of PS-*b*-P4VP and PS-*b*-P4VP (PBA) thin films. The GISAXS 2D patterns are shown in the left side whereas the in-plane profiles as a function q_y are shown in the right side of each image. Figure 5A shows a GISAXS 2D image along with the in-plane profile of 1,4 Dioxane solvent annealed block copolymer nanotemplate. The sharp Bragg rods (vertical streaks) in the GISAXS pattern correspond to the reflections from a 2D lattice of finite length oriented normal to the film surface. The reflections from the BC nanoporous thin film are located at scattering vectors of 1: $\sqrt{3}$: $\sqrt{4}$ relative to the first-order reflection, characteristic of hexagonally packed cylindrical microdomains. From the scattering vector of the primary reflection, the d-spacing was calculated to be 27 nm, which is consistent with the AFM and SEM observations. Figure 5B shows the GISAXS 2D image along with the in-plane intensity profile of the PS-b-P4VP / PBA supramolecular complex template. Similar to the BC nanoporous thin film, the extension of the scattering intensity along q_z direction again clearly indicates that the microstructures are oriented normal to the film surface. In this case, the reflections are located at the scattering vectors of 1: 2: 3 relative to the first-order reflection represent the lamellar microdomain morphology. The first-order peak at $q_y = 0.218\,\mathrm{nm}^{-1}$ corresponds to a spacing of 29 nm, which is consistent with the AFM and SEM results. The preferential orientation of the microdomain normal to the substrate in block copolymer thin film or SMC thin film is also supported by other literature.[16,18] Sidorenko *et al.*[16] demonstrated the reversible switching phenomena in a supramolecular complex based on PS-b-P4VP with HABA (2-(4′-hydroxybenzeneazo) benzoic acid) upon exposure to different solvents in thin film. This supramolecular complex provides perpendicular cylinders after annealing in 1,4-Dioxane and a reversible switching to parallel cylinders upon exposure to chloroform. In our case, we showed perpendicularly oriented lamellar microdomain of the SMC normal to the substrate in thin film upon solvent annealing in 1,4-Dioxane. The preferential orientation of the microdo-

mains can be attributed to the selectivity of the constituted blocks in that solvent[32] used for solution preparation and annealing. 1,4-Dioxane is a selective solvent for PS[18] not for P4VP or P4VP (PBA) block. So annealing in 1,4-Dioxane will induce the morphology of microdomains normal to the substrate. The morphology obtained upon evaporation of 1,4-Dioxane is of course, trapped in a nonequilibrium state. Heating the film above the glass transition temperature of the microdomain or annealing in a solvent which is almost equally selective for the both solvent will lead to the equilibrium state where microdomains are parallel to the surface.[18,33,34] Now it is important to discuss the reason for the change of the block copolymer thin film morphology after supramolecular assembly. The reason is obviously the composition change of the block copolymer film after the formation of supramolecular complex. The PBA molecules are associated with P4VP blocks by hydrogen bonding and behave like comb-like polymer chains as a whole. So the supramolecular assembly will effectively increase the block composition of P4VP due to the complexation with PBA through hydrogen bonding. Here, we used 1:1 molar ratio of P4VP and PBA for the formation of supramolecular assembly and this ratio allowed us to estimate the molecular weight of the PBA associated P4VP chain after the formation of supramolecular assembly. Here, in a first approximation, we can, assume that the supramolecular complex described here, can be treated like a modified diblock copolymer. The phase behaviour of the modified diblock copolymers (A-*b*-B) is dictated by the new Flory–Huggins segment–segment interaction parameter, χ, the degree of polymerization, N, which can be assumed stay constant and the volume fraction of the blocks (f_A and f_B) where the B block is increased in volume due to Hydrogen bonding. Matsen and Bates[35] demonstrate the phase diagram of block copolymer in between the weak ($\chi N \leq 10$) and strong ($\chi N \geq 10$) segregation regime. The diblock copolymer at $\chi \cdot N$ less than ca. 10.5 is always in disordered state disregarding the volume fraction of the blocks. From a random copolymer blend miscibility study, the χ value for the pure PS-*b*-P4VP diblock copolymer was determined to satisfy $0.30 < \chi_{PS\text{-}P4VP} \leq 0.35$ ($T \approx 160\,^{\circ}C$).[36,37] Very recently, a similar value of $0.317 < \chi_{PS\text{-}P4VP} \leq 0.347$ (T between 160 and 195 °C) was found from a diblock copolymer scattering study.[38] Such a large value implies the strong segregation limit of PS-*b*-P4VP for moderate molecular weight. The pure block copolymer gives cylindrical morphology as equilibrium structure after microphase separation at room temperature. Now after formation of the SMC, the presence of PBA might effectively decreases the χ parameter between PS and P4VP, while N stays constant, hence the χN value of the block copolymer will change accordingly, but still remains in the strong segregation regime. So the SMC should be in the ordered state at room temperature like the pure block copolymer. But the nature of the microphase separation is different, which resulting a change of the morphology of the block copolymer after SMC due to the increase of volume fraction of the P4VP (PBA). The qualitative phase diagram is shown in Figure 6. The region 1 in the phase diagram denotes pure block copolymer ($f_{PS} \approx 0.804$) having hexagonally arranged cylindrical morphology. After the formation of SMC with PBA, the block copolymer ($f_{PS} \approx 0.476$) goes to region 2 in the phase diagram with lamellar morphology.

Conclusion

In conclusion, we have described a novel supramolecular complex between poly(styrene)-*b*-poly(4-vinylpyridine) (PS-b-P4VP) and 1-pyrenebutyric acid (PBA) and have studied of its self assembly in thin film. The supramolecular complex of PS-b-P4VP and 1-pyrenebutyric acid changed the block copolymer morphology from cylindrical to lamella in thin film due to the increase of the volume fraction of P4VP

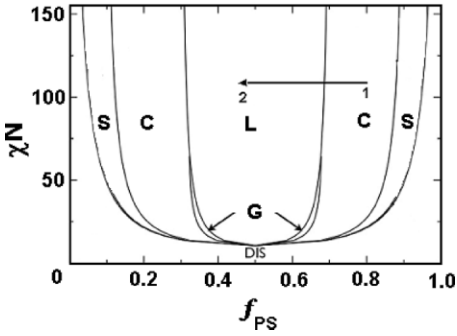

Figure 6.
Qualitative phase diagram of the block copolymer (PS-b-P4VP) and their supramolecular complex based on Masten and Bates diagram.[35] f_{PS} is the block fraction of polystyrene block, χ is the Flory-Huggins interaction parameter, and N is the length of the block. L = lamella, C = hexagonally packed cylinder, G = double gyroid, S = Sphere. The region 1 denotes pure block copolymer having hexagonally packed cylinder and region 2 denotes block copolymer vased supramolecular complex having lamellar structure.

(PBA). In both cases (parent block copolymer and SMC), the microdomains are oriented normal to the substrate after annealing in a selective solvent. Pure block copolymer shows cylindrical morphology with a periodicity ~26 nm, whereas the SMC shows lamellar morphology with a periodicity of ~ 29 nm. After fabricating the thin film from SMC, the minor component 1-pyrenebutyric acid can be easily removed by dissolving the thin film in ethanol to transform the block copolymer thin film into nanotemplate or membrane.

Acknowledgements: B. K. Kuila acknowledges financial support from Alexander von Humboldt Foundation. This research was also supported by the priority program of Deutsche Forschungsgemeinschaft (SPP1165, Project No. STA324/31). B. K. Kuila acknowledges E. B. Gowd for doing the GISAXS experiments. We thank HASYLAB, DESY, Hamburg, Germany for providing the facilities to use synchrotron radiation source for GISAXS experiments and BW4 beamline staff for the help in setting up the beam line at the HASYLAB.

[1] I. W. Hamely, *The physics of block copolymers*, Oxford University Press, New York **1998**.
[2] F. S. Bates, G. H. Fredrickson, *Annu. Rev. Phys. Chem.* **1990**, *41*, 525.
[3] (a) J. T. Chen, E. L. Thomas, C. K. Ober, G. P. Mao, *Science* **1996**, *272*, 343; (b) T. Thurn-Albrecht, J. Schotter, G. A. Kastle, N. Emley, T. Shibauchi, L. Krusin-Elbaum, K. Guarini, C. T. Black, M. T. Tuominen, T. P. Russell, *Science* **2000**, *290*, 2126.
[4] F. S. Bates, G. H. Fredrickson, *Phys. Today* **1999**, *52*, 32.
[5] (a) S. B. Darling, *Prog. Polym. Sci.* **2007**, *32*, 1152; (b) M. Ramanathan, E. Nettleton, S. B. Darling, *Thin Solid Films* **2009**, *517*, 4474; (c) A. Knoll, A. Horvat, K. S. Lyakhova, G. Krausch, G. J. A. Sevink, A. V. Zvelindovsky, R. Magerle, *Phys. Rev. Lett.* **2002**, *89*, 035501.
[6] R. A. Segalman, *Mater. Sci. Eng. R* **2005**, *48*, 191.
[7] C. J. Hawker, T. P. Russell, *MRS Bull.* **2005**, *30*, 952.
[8] T. L. Morkved, M. Lu, A. M. Urbas, E. E. Ehrichs, H. M. Jaeger, P. Mansky, T. P. Russell, *Science* **1996**, *16*, 931.
[9] (a) P. Mansky, P. M. Chaikin, E. L. Thomas, *J. Mater. Sci.* **1995**, *30*, 1987; (b) N. Haberkorn, M. C. Lechmann, B. H. Sohn, K. Char, J. S. Gutmann, P. Theato, *Macromol. Rapid commun.* **2009**, *30*, 1146.
[10] (a) M. Park, C. Harrison, P. M. Chaikin, R. A. Register, D. H. Adamson, *Science* **1997**, *276*, 1401; (b) K.-H. Lo, M.-C. Chen, R.-M. Ho, H.-W. Sung, *ACS Nano* **2009**, *3*, 2660.
[11] B. K. Kuila, B. Nandan, M. Böhme, A. Janke, *M. Stamm. Chem. Comm.* **2009**, 5749.
[12] B. K. Kuila, M. Stamm, *J. Mater. Chem.*, **2010**, *20*, 6086–6094.
[13] S. Valkama, T. Ruotsalainen, A. Nykanen, A. Laiho, H. Kosonen, G. ten Brinke, O. Ikkala, J. Ruokolainen, *Macromolecules* **2006**, *39*, 9327.
[14] J. Ruokolainen, M. Saariaho, O. Ikkala, G. ten Brinke, E. L. Thomas, M. Torkkeli, R. Serimaa, *Macromolecules* **1999**, *32*, 1152.
[15] O. Ikkala, G. ten Brinke, *Chem. Commun.* **2004**, 2131.
[16] A. Sidorenko, I. Tokarev, S. Minko, M. Stamm, *J. Am. Chem. Soc.* **2003**, *125*, 12211.
[17] W. van Zoelen, T. Asumaa, J. Ruokolainen, O. Ikkala, G. ten Brinke, *Macromolecules* **2008** *41*, 3199.
[18] I. Tokarev, R. Krenek, Y. Burkov, D. Schmeisser, A. Sidorenko, S. Minko, M. Stamm, *Macromolecules.* **2005**, *38*, 507.
[19] (a) H. Kosonen, J. Ruokolainen, M. Knaapila, M. Torkkeli, R. Serimaa, W. Bras, A. P. Monkman, G. ten Brinke, O. Ikkala, *Synth. Met.* **2001**, *121*, 1277; (b) G. A. van Ekenstein, E. Polushkin, H. Nijland, O. Ikkala, G. ten Brinke, *Macromolecules* **2003**, *36*, 3684.
[20] K. C. Wood, S. R. Little, R. Langer, P. T. Hammond, *Angew. Chem., Int. Ed.* **2005**, *44*, 6704.
[21] C. F. J. Faul, M. Antonietti, *Adv. Mater.* **2003**, *15*, 673.
[22] A. F. Thunemann, *Prog. Polym. Sci.* **2002**, *27*, 1473.
[23] S. Valkama, O. Lehtonen, K. Lappalainen, H. Kosenen, P. Castro, T. Repo, M. Torkelli,

R. Serimaa, G. ten Brinke, M. Leskela, O. Ikkala, *Macromol. Rapid Commun.* **2003**, *24*, 556.
[24] C. O. Osuji, C. Y. Chao, C. K. Ober, E. L. Thomas, *Macromolecules* **2006**, *39*, 3114.
[25] J. Ruokolainen, J. Tanner, G. ten Brinke, O. Ikkala, M. Torkelli, R. Serimaa, *Macromolecules*, **1995**, *28*, 7779.
[26] J. Ruokolainen, R. Makinen, M. Torkkeli, T. Makela, R. Serimaa, G. ten Brike, O. Ikkala, *Science* **1998**, *280*, 557.
[27] O. Ikkala, G. ten Brinke, *Science*, **2002**, *295*, 2407.
[28] S.-H. Tung, N. C. Kalarickal, J. W. Mays, T. Xu, *Macromolecules* **2008**, *41*, 6453.
[29] S.-H. Tung, T. Xu, *Macromolecules* **2009**, *42*, 5761.
[30] R. Krenek, PhD Thesis, Sächsische Landes- Staats- und Universitätsbibliothek (SLUB), Dresden **2007**.
[31] S. Park, J. Y. Wang, B. Kim, J. Xu, T. P. Russell, *ACS Nano* **2008**, *2*, 766.
[32] S. Park, J.-Y. Wang, B. Kim, W. Chen, T. P. Russell, *Macromolecules* **2007**, *40*, 9059.
[33] G. Kim, M. Libera, *Macromolecules* **1998**, *31*, 2569–2577.
[34] S. H. Kim, M. J. Misner, T. Xu, M. Kimura, T. P. Russell, *Adv. Mater.* **2004**, *16*, 226–231.
[35] M. W. Matsen, F. S. Bates, *Macromolecules* **1996**, *29*, 1091.
[36] G. O. R. Alberda van Ekenstein, R. Meyboom, G. ten Brinke, O. Ikkala, *Macromolecules* **2007**, *40*, 2109.
[37] W. van Zoelen, T. Asumaa, J. Ruokolainen, O. Ikkala, G. ten Brinke, *Macromolecules* **2008**, *41*, 3199.
[38] W. Zha, C. D. Han, D. H. Lee, S. H. Han, J. K. Kim, J. H. Kang, C. Park, *Macromolecules* **2007**, *40*, 2109.

